J. Chem. Sci. Vol. 129, No. 11, November 2017, pp. 1721–1734.
https://doi.org/10.1007/s12039-017-1384-1

REGULAR ARTICLE

Special Issue on Recent Trends in the Design and Development of Catalysts and their Applications

Preparation of TiO_2 supported Au–Pd and Cu–Pd by the combined strong electrostatic adsorption and electroless deposition for selective hydrogenation of acetylene

BOONTIDA PONGTHAWORNSAKUN, NISARAT WIMONSUPAKIT and JOONGJAI PANPRANOT*

Center of Excellence on Catalysis and Catalytic Reaction, Department of Chemical Engineering, Faculty of Engineering, Chulalongkorn University, Bangkok 10330, Thailand
E-mail: joongjai.p@chula.ac.th

MS received 8 April 2017; revised 18 August 2017; accepted 19 August 2017; published online 25 October 2017

Abstract. TiO_2 supported Au–Pd and Cu–Pd catalysts were prepared by strong electrostatic adsorption (SEA) of Pd followed by electroless deposition (ED) of a second metal with incremental surface coverages of Au or Cu. High dispersion of small Pd particles on the Pd/TiO_2 prepared by SEA led to the high amount of second metal deposition on Pd surface. The Cu addition by ED increased the relative ratio of linear CO adsorption mode indicating the presence of higher amount of isolated Pd atoms. The ensemble effect of the Cu–Pd/TiO_2 catalysts resulted in the improved catalytic performances in the selective hydrogenation of acetylene to ethylene. However, as revealed by the blue shift of CO-IR and XPS results, Au addition by ED rather exhibited the electronic modification. The highest catalytic activity was obtained on the 1.10% Au–Pd/TiO_2 catalyst; however, the Cu addition (0.12% Cu–Pd/TiO_2, $\theta_{Cu} = 0.37$) showed interesting results as only a small amount of Cu was used to improve the catalyst performances. The bimetallic catalysts were also prepared by conventional impregnation for comparison purposes. These catalysts exhibited several drawbacks such as low Pd dispersion, formation of second metal aggregates, and blockage of isolated Pd atoms.

Keywords. Bimetallic catalyst; Au–Pd/TiO_2; Cu–Pd/TiO_2; strong electrostatic adsorption; electroless deposition; selective hydrogenation of acetylene.

1. Introduction

In polymerization process, ethylene is considered as an initial point for polyethylene production. Typically, ethylene which is produced by steam cracking of higher hydrocarbons such as ethane, propane, butane, naphtha, and gas oil, contains a small quantity of acetylene (< 3%).[1,2] The acetylene contaminant should be removed to less than 5 ppm in polymerization grade ethylene feedstocks because it is poisonous to the catalyst for ethylene polymerization and then degrades the quality of polyethylene produced.[3–7] One of the methods for acetylene removal in ethylene streams is the selective hydrogenation of acetylene to ethylene by using supported Pd-based catalysts. Two important keys for this process are (i) ethylene selectivity, which is the fraction of acetylene conversion to ethylene, and (ii) catalyst lifetime, which is limited by oligomers deposition during the reaction.[8,9] Conventional, supported Pd-based catalysts have been used to catalyze the selective hydrogenation of acetylene.[10–12] However, the drawback of Pd-based catalysts is the strong adsorption of both reactants and products on Pd metal, leading to low ethylene selectivity in spite of high acetylene conversion.[13] In order to reduce contact of Pd with reactants and products, second metals such as Au, Cu, Ag, Ga, Ti, Nb, and Ce have been added to dilute Pd metal surface.[2,6,14–19]

The role of second metal addition is generally classified into two factors consisting of geometric and electronic effects. For example, Cu addition by inserting Cu into Pd matrix was found to decrease the number of multi-coordination Pd sites responsible for dissociative adsorption of acetylene.[15] As a result, ethylene hydrogenation was suppressed due to geometric effect, leading to higher ethylene selectivity. Pei *et al.*,[20]

*For correspondence

reported the improvement of ethylene selectivity at high acetylene conversion upon Cu addition due to both of geometric and electronic effects, suggesting that the isolation of Pd by Cu and the electron transfer from Cu to Pd resulted in the weak adsorption of ethylene and promoted H_2 dissociation. The effect of second metal addition is also dependent on the catalyst preparation method. Kim *et al.*,[21] reported that the Cu addition into Pd by a surface redox method exhibited higher acetylene conversion and ethylene selectivity than those prepared by incipient wetness impregnation because the former method resulted in the intimate contact between the promoter and Pd surface and then led to the modification of electronic structure of Pd surface by increasing the electron density of Pd, thus improving the ethylene selectivity. Choudhary *et al.*,[14] found that Au addition by impregnation/deposition precipitation resulted in the presence of individual Pd and Au particles indicating no interaction between two metals. Unlike the impregnation/deposition precipitation method, the bimetallic Au–Pd/TiO_2 preparation by redox method led to the close interaction of Au and Pd. The other drawbacks of conventional preparation include the lack of homogeneity in particle size and shape in both monometallic and bimetallic catalysts and the random distribution of compositions of the two metals.[22,23]

Strong electrostatic adsorption (SEA) is a special case of wet impregnation that results in monolayer adsorption of metal complexes on the support surface[24–27] and provides higher metal dispersion compared to the conventional incipient wetness impregnation.[25] For the preparation of bimetallic catalysts by electroless deposition (ED) method, the reducible metal salt (secondary metal) is selectively deposited onto the catalytically active sites (monometallic primary metal) through a controlled chemical reaction with a liquid-phase reducing agent. The advantage of ED is the selective deposition of controlled amounts of the secondary metal on the catalyst surface without the formation of isolated crystallites of the secondary metal on a catalyst support. In our recent study, the combined SEA-ED method was employed for the preparation of the bimetallic Ag–Pd/TiO_2 catalysts.[7] The dilution of Pd sites by Ag addition was found to facilitate acetylene adsorption as π-bonded species, leading to the improvement of ethylene selectivity in the selective hydrogenation of acetylene.

In this study, the use of combined SEA-ED method was extended for the preparation of the bimetallic Au–Pd/TiO_2 and Cu–Pd/TiO_2 catalysts. The Pd/TiO_2 was prepared by SEA first and then the second metal was added by ED with incremental surface coverages of Au or Cu. The catalysts were characterized by various analytical methods such as inductively-coupled plasma optical emission spectroscopy (ICP-OES), X-ray diffraction (XRD), Chemisorption using H_2 titration, Fourier transfer infrared (FTIR) of adsorbed CO, X-ray photoelectron spectroscopy (XPS), and transmission electron spectroscopy (TEM). Their catalytic performances were tested in the gas-phase selective hydrogenation of acetylene.

2. Experimental

2.1 *Catalyst preparation*

2.1a *Preparation of the Pd/TiO_2 catalyst by SEA method*: The Pd/TiO_2 catalyst was prepared by SEA method according to the procedure described in Riyapan *et al.*[7] Firstly, the point of zero charge (PZC) of the support, which is the pH value at which the electrical charge density on the support surface is zero, must be determined. The PZC of TiO_2 was determined by using the method of Regalbuto.[25,28,29] The commercial titanium dioxide (99.7%, Sigma Aldrich, China) with a surface area of 50 m^2/g was used as the support in this study. Water solutions were prepared at various initial pH values in the range of 1 to 12 with HCl (37%, RCI Labscan, Thailand) and NaOH (≥ 99%, Merck, Germany). Then, the TiO_2 supports were added into the solutions and shaken for 1 h. After stabilization, the final pH was measured. The plot of the final pH vs the initial pH, also called as pH shift plot, was obtained and the plateau of this plot indicated to the PZC of TiO_2 supports. The total TiO_2 surface area in solution (surface loading) was fixed to be equal to 1000 m^2/L. According to the pH shift plot of the TiO_2 support, as shown in Figure 1, the PZC value of the TiO_2 was found to be 5.45 corresponding to the final pH value of the plateau.

In this study, palladium (II) tetraammine chloride monohydrate ($Pd(NH_3)_4Cl_2 \cdot H_2O$, ≥ 99.99%, Aldrich, USA) was used as the Pd precursor. Based on the PZC of the TiO_2 at 5.45, the $[Pd(NH_3)_4]^{2+}$ cation from the Pd precursor would be adsorbed at pH values above its PZC. Thus, the Pd uptake-pH survey (adsorption survey) was conducted in

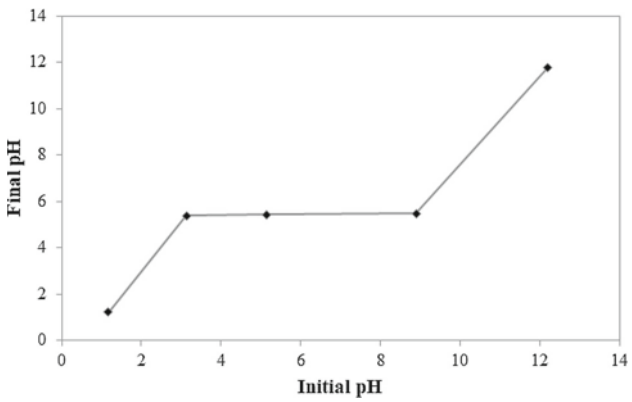

Figure 1. pH shift plot of the TiO_2 support.

the pH region above 5.45 in order to determine the pH of strongest interaction. The $Pd(NH_3)_4Cl_2$ solution was made up at 200 ppm and then adjusted the initial pH with NaOH in the range of 9–12 for the adsorption of $[Pd(NH_3)_4]^{2+}$ over TiO_2 support. The prepared $Pd(NH_3)_4Cl_2$ solutions were considered as the pre-contacted solutions and then the Pd concentration was determined by ICP-OES technique. After that, TiO_2 was weighed to obtain the surface loading of 1000 m^2/L and added into 200 ppm of $Pd(NH_3)_4Cl_2$ solution. The TiO_2 slurries in $Pd(NH_3)_4Cl_2$ solutions were shaken for 1 h and then measured the final pH of these slurries. Two ml of each slurry solution was withdrawn and filtered in order to analyze the Pd concentration in the post-contacted solution. The Pd uptake at various pH values was calculated form the difference in the Pd concentration between the pre-contacted and post-contacted solutions.

The Pd surface density, Γ, was determined from the concentration of Pd adsorbed divided by the surface loading as follows:

$$\Gamma_{metal} = \frac{\left(C_{metal,initial} - C_{metal,final}\right)}{Surface\ loading}$$

The adsorption curve in the term of Pd surface density as a function of the final pH is shown in Figure 2. The maximum Pd adsorption on TiO_2 support was reached at the final pH of 11.3 (initial pH = 11.8). A large batch of the Pd/TiO_2 catalyst was prepared by adjusting the initial pH (prior to Pd deposition) which corresponded to the required amount of Pd adsorption. The surface loading was still maintained at 1000 m^2/L. The slurry solution was shaken for 1 h and subsequently filtered. The pre-contacted and post-contacted solution were used to determine the Pd metal loading by ICP-OES; in addition, the recovered solid was dried for 12 h. Finally, the Pd/TiO_2 catalyst prepared was reduced with H_2 at 200°C for 2 h. The amount of Pd loading for the obtained Pd/TiO_2 catalyst prepared by SEA was found to be 1.29 wt%.

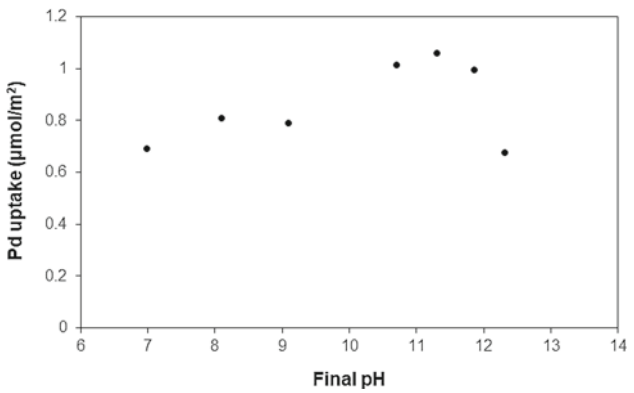

Figure 2. Adsorption curve in the term of Pd surface density as a function of the final pH.

2.1b *Preparation of the bimetallic Au–Pd/TiO$_2$ and Cu–Pd/TiO$_2$ catalysts by using ED method*: The 1.29 wt% Pd/TiO_2 catalyst prepared by SEA was used to prepare the bimetallic Au–Pd/TiO_2 and Cu–Pd/TiO_2 catalysts by ED method. The dispersion of Pd was investigated by hydrogen titration of oxygen pre-covered Pd sites with using a Micromeritics ChemiSorb 2750 automated system as described in the catalyst characterization. The Pd dispersion for 1.29 wt% Pd/TiO_2 was found to be 37.9% which corresponded to 2.76×10^{19} surface Pd sites/g of catalyst. The cyanide metal precursors including gold cyanide $[Au(CN)_2^-]$ from potassium dicyanoaurate ($KAu(CN)_2$, 98%, Aldrich, USA) and copper cyanide $[Cu(CN)_2^-]$ from potassium dicyanocuprate ($KCu(CN)_2$, 100%, STREM Chemicals, USA) were used as Au and Cu precursors for the synthesis of the bimetallic Au–Pd/TiO_2 and Cu–Pd/TiO_2 catalysts, respectively. The molar ratio of metal salt/reducing agent was initially 1:10 in which hydrazine (N_2H_4, 35 wt% in H_2O, Aldrich, Germany) and dimethylamineborane ($(CH_3)_2NH \cdot BH_3$; DMAB, 97%, Aldrich, Russian Fed) were used as the reducing agent for Au and Cu deposition, respectively. Initial concentrations of the metal salts were selected based on the desired theoretical coverage of Au or Cu on Pd, assuming monolayer deposition and 1:1 surface stoichiometry of Au or Cu deposited on Pd.

A series of bimetallic Au–Pd/TiO_2 and Cu–Pd/TiO_2 catalysts with various Au or Cu coverages on Pd was synthesized by ED method. During ED, the bath for the deposition of Au was continuously stirred at room temperature; while the bath for the deposition of Cu was carried out at 40°C. The pH of bath solution was adjusted to maintain at 9.0 ± 0.5 by dropwise addition of sodium hydroxide (NaOH). The liquid samples of ED solution were periodically withdrawn at various deposition time and filtered with a syringe filter in order to remove the solid catalyst before ICP-OES analysis to measure the metal cyanide ($Au(CN)_2^-$ or $Cu(CN)_2^-$) concentration remaining in the bath solution. After 1 h of deposition time, the ED solution was filtered and the solid catalyst was washed repeatedly with deionized water to remove all soluble ligands and salts. After that, the samples were dried under vacuum at room temperature and stored at ambient conditions.

2.1c *Preparation of the bimetallic Au–Pd/TiO$_2$ and Cu–Pd/TiO$_2$ catalysts by impregnation (IM) method*: The 1.29 wt% Pd/TiO_2 catalyst prepared by SEA was used to prepare the bimetallic Au–Pd/TiO_2 and Cu–Pd/TiO_2 catalysts by IM method. The gold (III) chloride trihydrate ($HAuCl_4 \cdot 3H_2O$, $\geq$ 99.9%, Aldrich, USA) and copper (II) nitrate trihydrate ($Cu(NO_3)_2 \cdot 3H_2O$, 100%, Aldrich, USA) were used as Au and Cu precursors, respectively. The 1.29 wt% Pd/TiO_2 catalyst was impregnated with the precursor solution of second metal, dried at 110 °C overnight, and calcined in air at 350 °C for the Au–Pd/TiO_2 and 450 °C for the Cu–Pd/TiO_2 for 3 h. These bimetallic Au–Pd/TiO_2 and Cu–Pd/TiO_2 catalysts prepared by incipient wetness impregnation are denoted as Au–Pd/TiO_2 (IM) and Cu–Pd/TiO_2 (IM), respectively.

2.2 *Catalyst characterization*

The concentration of metal during the catalyst preparation by strong electroless adsorption and electroless deposition was analyzed by ICP-OES technique using the Perkin Elmer Optima 2100 DV spectrometer (USA). The XRD patterns were recorded from 20 to 80° by using a Bruker D8 Advance X-ray diffractometer (USA) connected with a computer with Diffract ZT version 3.3 programs. The XPS was performed on a Kratos AMICUS X-ray photoelectron spectrometer (UK) using MgK_α X-ray radiation and equipped with Kratos VISION2 software. The XPS spectra were collected at 0.1 eV energy step size and 75 eV pass energy. The C 1s line was used as the internal standard at binding energy of 285.0 eV. The TEM micrographs of the catalysts were analyzed by using a JEOL-JEM 2001 CX transmission electron microscope (USA) operated at 100 kV.

The CO adsorbed on the metal surface was measured by using Bruker FTIR spectrometer (USA) with a liquid nitrogen-cooled MCT detector. The pellets of 1.5 cm diameter were prepared by pressing ~ 0.05 g of sample at 6000 lb force and then placed in a temperature-controlled flow cell. Before to analyze, the He gas was introduced into the sample cell in order to remove the remaining air and the sample was reduced in H_2 for 1 h at 200 °C, and then cooled down to 30 °C. After that, the pellet was exposed to CO for 15 min and then purged with He gas. The FTIR spectra were recorded in the range of 400–4000 cm^{-1} at a wavenumber resolution of 4 cm^{-1} and 150 scans.

Chemisorption using hydrogen pulse titration of oxygen-precovered Pd was conducted by using a Micromeritics ChemiSorb 2750 automated system (USA) attached with ChemiSoft TPx software. Prior to titration, approximately 0.05 g of catalyst was reduced in flowing pure H_2 at 200 °C for 2 h and then purged with pure Ar for 1 h at 200 °C to remove chemisorbed hydrogen from the metal surface. After cooling to 40 °C under Ar flowing, the sample was exposed to 1% O_2/balance He for 30 min to saturate the Pd surface with adsorbed atomic oxygen forming the Pd–O species at surface. After that, the pure Ar was introduced for 30 min to remove the residual O_2. Then, the pure H_2 was pulse introduced until no further H_2 uptake was observed which means that all adsorbed atomic oxygen of Pd–O surface species reacts with the pure H_2 pulse to form H_2O and then the adsorbed atomic oxygen was replaced with the atomic hydrogen. The quantitative hydrogen consumption was determined by using a high sensitivity thermal conductivity detector (TCD) below the sample cell. The H_2 pulse titration was analyzed based on the equation of $1.5\ H_2 + Pd{-}O \rightarrow H_2O + Pd{-}H$. This equation assumed that H_2 rapidly reacts with adsorbed O atoms to form H_2O and to cover the vacant Pd site with atomic H without formation of β-palladium hydride. Thus, the stoichiometry of hydrogen adsorption was 1.5 H_2: Pd. Based on the inactive of Au and Cu for hydrogen–oxygen titration at 40 °C, the concentration of Pd surface sites which were covered by Au or Cu metals can be calculated by subtracting the Pd surface site concentration of the bimetallic catalysts from the total number of surface Pd sites of the monometallic Pd/TiO_2 catalyst.

2.3 *Reaction study*

The selective hydrogenation of acetylene in excess ethylene was investigated at the temperature in the range of 40–100°C. Approximately 0.15 g of catalyst was packed in a pyrex tubular downflow reactor (i.d. 10 mm). Before to test the reaction, the catalyst was reduced with H_2 at 150 °C for 2 h and then cooled down under Ar to the initial reaction temperature. The feed gases containing 1.5% C_2H_2, 1.7% H_2, and balance C_2H_4 was introduced into the reactor at the temperature of 40 °C and 1 atm. Each reaction temperature was kept constant for 1 h before increasing to the next point. The feed composition and gas mixture product at the outlet of reactor were analyzed by a gas chromatograph equipped with a flame ionization detector (SHIMADZU FID GC 8APF, Carbosieve column S-II) in order to detect the C_2H_2, C_2H_4, and C_2H_6 and a gas chromatograph equipped a thermal conductivity detector (SHIMADZU TCD GC 8APT, Molecular sieve 5A) in order to analyze the H_2.

Since the hydrogenation of acetylene was performed in the excess ethylene, change in ethylene could not be detected accurately enough. Thus, the selectivity to ethylene was determined based on the ethane formation.[30] The acetylene conversion and selectivity to ethylene were calculated as follows:[13,30–32]

$$\text{Acetylene conversion} = \frac{C_2H_2(\text{feed}) - C_2H_2\ (\text{out})}{C_2H_2(\text{feed})} \times 100\%$$

$$\text{Ethylene selectivity} = \left(1 - \frac{C_2H_6\ \text{formed}}{C_2H_2\ \text{converted}}\right) \times 100\%$$

3. Results and Discussion

3.1 *Catalyst characterization*

The XRD patterns of commercial TiO_2 support, the monometallic 1.29 wt% Pd/TiO_2 catalyst (after reduction) prepared by SEA, and the bimetallic Au–Pd/TiO_2 and Cu–Pd/TiO_2 catalysts prepared by ED and IM are shown in Figure 3. All samples showed the XRD characteristics peaks of anatase TiO_2 at 2θ degrees = 25° (major), 37°, 48°, 54°, 56°, 62°, 69°, 70° and 75°.[33,34] The diffraction peaks for Pd or PdO were not detected probably because of low content of Pd loading and/or well-dispersed of Pd nanoparticles on TiO_2 support.[23,35,36] The average crystallite sizes of anatase TiO_2 were calculated to be in the range of 15–17 nm for all the samples. There were no changes in the crystalline phase and average crystallite size of TiO_2 after loading of the metal (Pd, Au, or Cu).

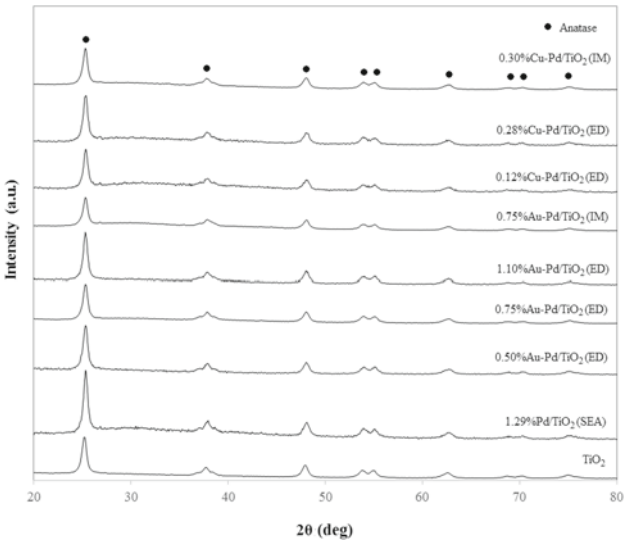

Figure 3. XRD patterns for commercial TiO_2 support, Pd/TiO_2, Au−Pd/TiO_2, and Cu–Pd/TiO_2 catalysts.

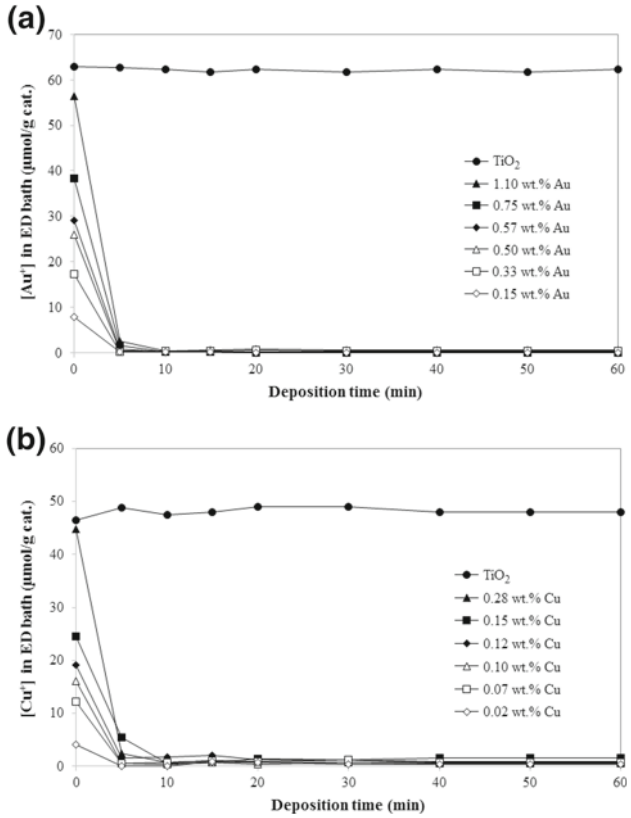

Figure 4. Time dependent metal deposition profiles of (a) Au and (b) Cu deposition.

The kinetics of Au and Cu deposition for the series of bimetallic Au–Pd/TiO_2 and Cu–Pd/TiO_2 catalysts prepared by ED with incremental coverage of the second metal on Pd surface are shown in Figure 4. It is confirmed that Au and Cu were not directly deposited on the TiO_2 support (no change in the deposition curve of TiO_2). The Pd surface was required for catalytic activation of the reducing agents as shown by the deposition curve of the Pd/TiO_2 in which the concentration of metal cyanide decreased with deposition time and a complete deposition was reached within 10 min.

The dispersion of Pd on the Pd/TiO_2 and the bimetallic Au–Pd/TiO_2 and Cu–Pd/TiO_2 catalysts were evaluated by using H_2 titration of O-precovered Pd surface sites based on the inactivation of the second metals (Au and Cu) as given in Table 1. The Pd dispersion for 1.29 wt% Pd/TiO_2 was found to be 37.9%, which corresponded to 2.76×10^{19} Pd surface sites/g of catalyst. Increasing of the second metal deposition, Pd dispersion decreased indicating the partial blockage of Pd sites by the deposition of the second metals. The ICP results of ED baths and filtrates confirmed that there was no Pd metal leaching or Pd dissolution by free CN^- ligands after deposition.[37] Moreover, sintering of Pd particles due to the effect of reducing agent has been reported to be negligible under typical ED conditions.[38] Based on the deposition curve in Figure 4 and the second metal coverage in Table 1, increasing of Au more than 40 $\mu mol/g_{cat}$ and Cu more than 25 $\mu mol/g_{cat}$ resulted in little increase of deposition of the second metals, suggesting that most of the Pd surface may be covered by the second metals and the second metals were much less active than Pd for activation of the reducing agents. Compared to the bimetallic Au–Pd/TiO_2 and Cu–Pd/TiO_2 catalysts prepared by the conventional impregnation, the bimetallic prepared by SEA-ED showed higher coverage of the second metal for a similar loading.

The deviations of exposed Pd sites from the theoretical straight line (solid line) for monodispersed coverage of second metals on the Pd surface at 1:1 deposition stoichiometry are illustrated in Figure 5. The beginning point for the deviation of the actual coverage from the theoretical coverage pointed nearly complete coverage of the second metal on the Pd surface and suggested that the autocatalytic deposition of the second metal occurred. For low loading of the second metal, the catalytic deposition of the second metal on Pd surface predominated because the hydrazine is preferentially activated on Pd compared to Au as well as the dimethylamineborane which is preferentially activated on Pd compared to Cu.[37,39] The actual Au coverage began to deviate from the theoretical Au coverage at $\theta_{Au} = 0.20$, which indicated the beginning of the autocatalytic deposition of Au on Au. The autocatalytic deposition of Cu on Cu was observed at $\theta_{Cu} = 0.50$. Nevertheless, compared to the values reported previously by Rebelli *et al.*,[37] for the preparation of Au- and Cu−Pd/SiO_2 catalysts by ED method on a commercial Pd/SiO_2 with 8.6%

Table 1. Chemisorption results using H_2 titration of O-pre-covered Pd surface sites for Pd/TiO_2, $Au-Pd/TiO_2$, and $Cu–Pd/TiO_2$ catalysts.

Sample	Dispersion (%)	Theoretical coverage (ML)	Actual coverage (ML)
1.29%Pd/TiO_2	37.9	–	–
0.15%$Au-Pd/TiO_2$(ED)	32.5	0.17	0.14
0.33%$Au-Pd/TiO_2$(ED)	32.2	0.37	0.15
0.50%$Au-Pd/TiO_2$(ED)	26.3	0.55	0.31
0.57%$Au-Pd/TiO_2$(ED)	23.5	0.63	0.38
0.75%$Au-Pd/TiO_2$(ED)	17.1	0.83	0.55
1.10%$Au-Pd/TiO_2$(ED)	15.6	1.22	0.59
0.75%$Au-Pd/TiO_2$(IM)	32.3	0.83	0.15
0.02%$Cu-Pd/TiO_2$(ED)	35.6	0.07	0.06
0.07%$Cu-Pd/TiO_2$(ED)	34.5	0.24	0.09
0.10%$Cu-Pd/TiO_2$(ED)	26.5	0.34	0.30
0.12%$Cu-Pd/TiO_2$(ED)	23.9	0.41	0.37
0.15%$Cu-Pd/TiO_2$(ED)	18.9	0.52	0.50
0.28%$Cu-Pd/TiO_2$(ED)	17.4	0.96	0.54
0.30%$Cu-Pd/TiO_2$(IM)	28.7	1.03	0.24

*The theoretical coverage referred to theoretical monodisperse layer (ML) of Au or Cu on Pd

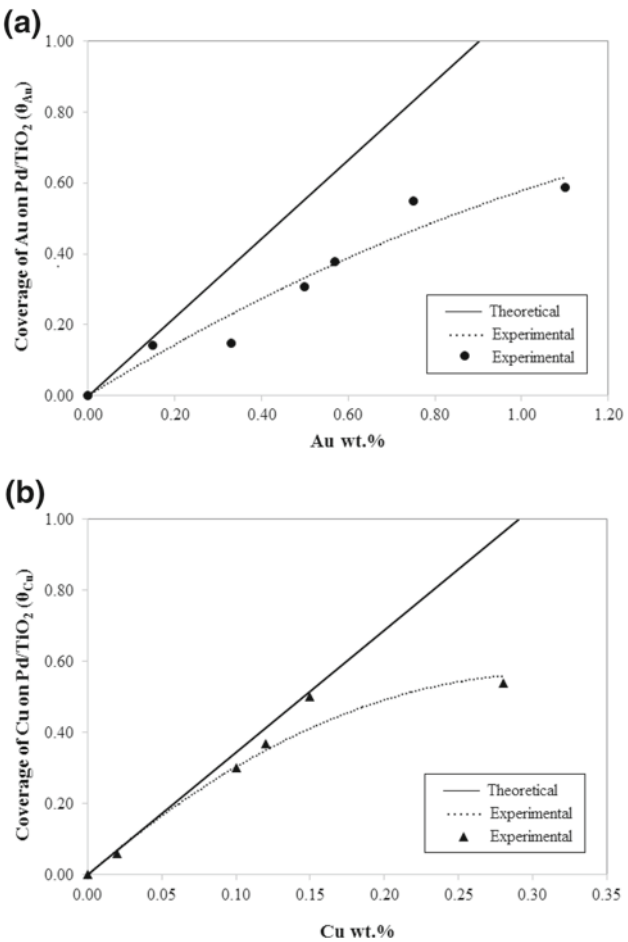

Figure 5. Actual coverage of second metal on Pd/TiO_2 as a function of weight of second metal deposition for (a) $Au–Pd/TiO_2$, and (b) $Cu–Pd/TiO_2$ catalysts.

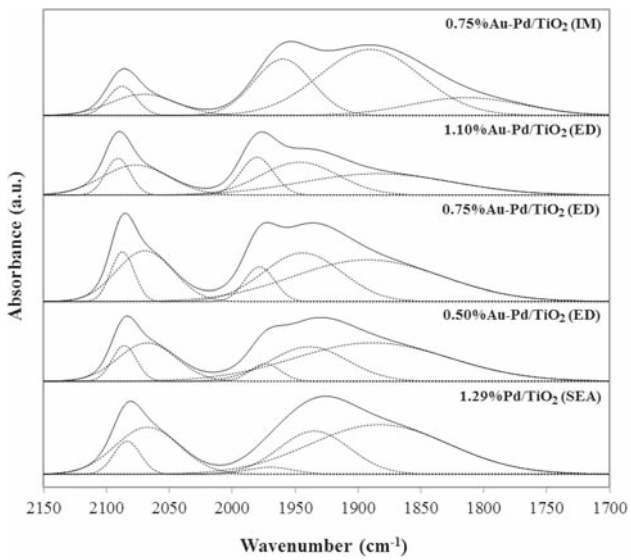

Figure 6. FTIR spectra of CO adsorbed on Pd sites for Pd/TiO_2 and $Au–Pd/TiO_2$ catalysts.

Pd dispersion, the autocatalytic deposition of Au and Cu was found at 0.16 wt% and 0.08 wt%, respectively. It has been suggested that the autocatalytic deposition could be delayed on the high dispersion Pd catalysts.[7]

The FTIR spectroscopy of CO adsorbed on Pd sites was performed at 30 °C for both the monometallic Pd/TiO_2 and bimetallic $Au–Pd/TiO_2$ and $Cu–Pd/TiO_2$ catalysts and the results are shown in Figures 6 and 7, respectively and also summarized in Table 2. For the monometallic Pd/TiO_2, the CO stretching bands were

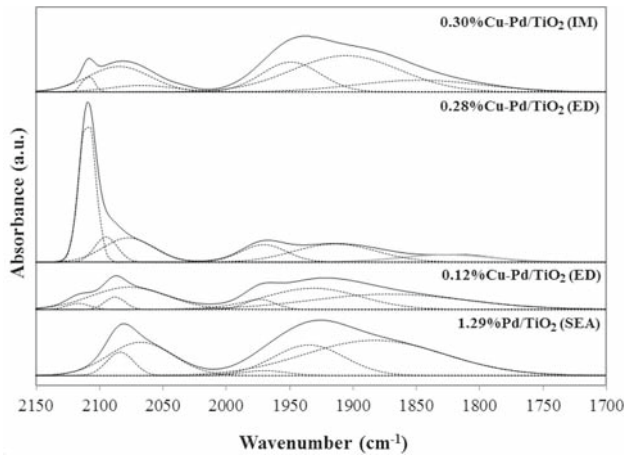

Figure 7. FTIR spectra of CO adsorbed on Pd sites for Pd/TiO$_2$ and Cu–Pd/TiO$_2$ catalysts.

resolved into 2 regions consisting of 2000–2100 cm^{-1} and 1800–2000 cm^{-1} regions. The former region was assigned to the adsorbed linear CO on Pd sites whereas the later was assigned to the adsorbed bridged and multi-coordinated CO on Pd sites.[40] Those in the linear region could be further deconvoluted into 2 peaks in the range of 2077–2100 cm^{-1} (L1) and 2068–2074 cm^{-1} (L2), which were attributed to the linearly bonded CO molecules on defects of low coordination sites such as corners, steps and kinks of Pd(1 1 1) and Pd(1 0 0) surfaces, respectively.[41,42] The nonlinear region observed in the range of 1800–2000 cm^{-1} could be deconvoluted into 3 peaks corresponding to the three modes of multiply-bound adsorption of CO on Pd sites: compressed-bridged (NL1), isolated-bridged (NL2) and tri-coordinated (NL3) modes.[43] The IR bands corresponding to CO adsorbed on Pd in the compressed-bridged, isolated-bridged and tri-coordinated modes were reported at wavenumbers 1995–1975, 1960–1925, and 1890–1870 cm^{-1}, respectively.[43] The bridged bond CO adsorbed on defect sites such as particle edges and corners were observed at 1960 cm^{-1},[43,44] while the bands around 1930–1970 cm^{-1} and 1970–2000 cm^{-1} were assigned to bridged bonded species on the terraces of the aggregates and the edges of the aggregates, respectively.[45] Furthermore, the specific two-fold bridged bond CO on low index planes such as Pd(1 1 0) and Pd(1 0 0) could be found at peaks 1978 and 1938 cm^{-1}, respectively.[40,46,47] In addition, the specific three-fold hollow sites of CO adsorption on Pd(1 1 1) surfaces were consistent with the peaks at 1876 and 1812 cm^{-1}.[40,48] The CO-IR spectra of the bimetallic catalysts can be interpreted by both ligand and ensemble effects. The ligand effect influences the position of the high-frequency bands; in addition, the ensemble effect

Table 2. FTIR of adsorbed CO peak position and intensity ratio for Pd/TiO$_2$, Au–Pd/TiO$_2$, and Cu–Pd/TiO$_2$ catalysts.

Samples	ML on Pd	Cu/Cu$^+$	Linear region(L)		Bridge region(NL)			Linear/Bridge	L/(L+NL)
			L1	L2	NL1	NL2	NL3		
1.29%Pd/TiO$_2$	–	–	2083 (0.06)	2067 (0.21)	1970 (0.02)	1934 (0.21)	1882 (0.49)	0.382	0.28
0.50%Au–Pd/TiO$_2$(ED)	0.31	–	2085 (0.07)	2067 (0.18)	1973 (0.04)	1938 (0.22)	1888 (0.49)	0.330	0.25
0.75%Au–Pd/TiO$_2$(ED)	0.55	–	2087 (0.08)	2069 (0.19)	1978 (0.07)	1944 (0.25)	1892 (0.41)	0.366	0.27
1.10%Au–Pd/TiO$_2$(ED)	0.59	–	2090 (0.09)	2076 (0.20)	1980 (0.13)	1946 (0.26)	1884 (0.32)	0.417	0.29
0.75%Au–Pd/TiO$_2$(IM)	0.15	–	2087 (0.06)	2070 (0.10)	1959 (0.23)	1890 (0.47)	1813 (0.14)	0.185	0.16
0.12%Cu–Pd/TiO$_2$(ED)	0.37	2116	2087 (0.04)	2076 (0.26)	1973 (0.05)	1931 (0.30)	1871 (0.36)	0.416	0.29
0.28%Cu–Pd/TiO$_2$(ED)	0.54	2109	2094 (0.12)	2077 (0.26)	1970 (0.17)	1913 (0.31)	1826 (0.14)	0.600	0.38
0.30%Cu–Pd/TiO$_2$(IM)	0.24	2108	2084 (0.17)	2066 (0.05)	1948 (0.19)	1905 (0.43)	1848 (0.16)	0.280	0.22

influences the intensity of these same bands. For the FTIR spectra of the bimetallic Au–Pd/TiO_2 catalysts, all the catalysts showed both linear and bridged CO-Pd adsorption bands. Meanwhile, the CO adsorption for the monometallic Au was reported to be negligible.[37,49] The relative intensity ratio of linear CO adsorption was not significantly changed with Au deposition. On the other hand, it was found that the relative intensity ratio of tri-coordinated (NL3) adsorption modes decreased, while the relative intensity ratios of compressed-bridged (NL1) and isolated-bridged (NL2) increased upon ED of Au on Pd because of dilution of Pd surface by deposition of Au confirming the coverage of Pd surface by ED of Au. Such results suggest the selective deposition of Au on the three-fold hollow sites on Pd surfaces. The bimetallic Au–Pd/TiO_2 catalysts prepared by impregnation showed the linearly adsorbed CO on Pd (1 1 1) and Pd(1 0 0) surfaces at 2087 and 2070 cm^{-1}, the band for two-fold bridged bond CO at 1959 cm^{-1}, and two bands for the three-fold hollow sites of CO adsorption on Pd at 1890 and 1813 cm^{-1}. The decrease in relative intensity of linear band (L2) was consistent with more coverage on isolated Pd (100) sites by Au. Among the prepared catalysts, the relative ratio of linear to nonlinear CO adsorption modes was lowest for the Au addition by impregnation method.

According to the FTIR spectra of the bimetallic Cu–Pd/TiO_2 catalysts, the linear and bridged CO-Pd adsorption bands were apparent in addition to the moderately strong peak at 2130–2110 cm^{-1} which was attributed to CO adsorption on Cu and/or Cu^+ sites.[50–52] For the bimetallic Cu–Pd/TiO_2 catalysts prepared by ED, the intensities of bridged bands significantly decreased with increasing Cu deposition (as shown in Figure 7) indicating the dilution of Pd surface by deposition of Cu. The results are consistent with an increasing of the intensities of CO−Cu/Cu^+ bands. The relative intensities of linear and two-fold bridged bond CO adsorption increased, but the relative intensity of tri-coordinated CO adsorption modes decreased after Cu deposition, also indicating that the ED of Cu was selectively occurred on three-fold hollow sites of Pd surfaces. The relative intensities of linear to bridged peaks (L/NL) were found to increase after addition of Cu by ED. The bimetallic Cu–Pd/TiO_2 catalysts prepared by impregnation showed adsorbed linear CO on Pd sites, which appeared at 2084 and 2066 cm^{-1} corresponding to adsorbed CO on Pd(1 1 1) and Pd(1 0 0) surfaces, one band for two-fold bridged bond CO at 1948 cm^{-1}, and two bands for three-fold hollow sites of CO adsorption on Pd at 1905 and 1848 cm^{-1}. The relative intensity of linear band at 2066 cm^{-1} (L2) was largely decreased, while the relative intensity of another linear band was found to be increased. The relative ratio of linear to nonlinear adsorption modes after Cu addition by IM was found to be lower than the Pd/TiO_2 catalysts similar to the results of Au addition by IM. Thus, it could be concluded that the second metal addition by IM method resulted in the major deposition of second metal on the isolated Pd sites.

The effect of second metal deposition by ED method on the promotion of isolated Pd atoms was somewhat different from those reported previously by Rebelli *et al.*[37] Due probably to the low dispersion of their starting Pd/SiO_2 catalysts (8.6% dispersion), the addition of second metal by ED resulted in an increase of the relative intensity of linear to bridged peaks. Whilst in this work, the deposition of second metal by ED on Pd/TiO_2 catalysts with high dispersion resulted in a decrease of the linear band due to coverage of isolated Pd sites by the second metal. Thus, the creation of isolated Pd atoms by second metal addition not only depended on the nature of Pd but also depended on the preparation method and the amount of second metal loading.

Considering the band positions, the FTIR spectra of the linear and non-linear bands shifted to higher frequencies upon Au deposition, indicating a blue shift compared to the Pd/TiO_2, suggesting the presence of electronic effect between Pd and Au (i.e., electron transfer from Pd to Au). According to the literature, both red and blue shifts could be found in bimetallic Au-Pd catalysts.[49,53–55] The red shift was observed when the effect of Pd dilution outweighed the blue shift due to electronic modification of Pd by Au as reported by Rebelli *et al.*[37] The linear band of the Cu–Pd/TiO_2 catalysts also showed a blue shift due to the electronic effect between Pd and Cu similar to Rebelli *et al.*,[37] whereas the non-linear band was found to be shifted to lower frequencies (red shift) relative to the Pd/TiO_2 catalysts. It is suggested that Cu was selectively deposited on contiguous Pd, leading to the creation of isolated Pd atoms. As a consequence, the intensity of non-linear bands was obviously decreased and the relative ratio of linear to non-linear bands was changed upon Cu deposition. It should also be noted that when the second metal was added by IM method, the effect of Pd dilution appeared to outweigh the electronic effect.

The XPS results including the binding energies of $Pd3d_{5/2}$ and $Au4f_{7/2}$ are summarized in Table 3. The XPS signals of Cu could not be clearly seen because of very low loading of Cu. Typically, the binding energy of Pd and Au metals was reported to be in the range of 335.0–335.4 eV[56] and 83.8–84.0 eV,[57] respectively. The monometallic Pd/TiO_2 showed one species of Pd oxides at 335.6 eV, while the peak of $Pd3d_{5/2}$ spectra for the bimetallic Au–Pd/TiO_2 catalysts could be deconvoluted into 2 peaks with FWHM < 2 indicating to two species

Table 3. Binding energy of Pd3d$_{5/2}$ and Au4f$_{7/2}$ for Pd/TiO$_2$, Au−Pd/TiO$_2$, and Cu–Pd/TiO$_2$ catalysts.

Samples	Pd3d$_{5/2}$				Au4f$_{7/2}$	
	B.E. (eV)	FWHM	B.E. (eV)	FWHM	B.E. (eV)	FWHM
1.29%Pd/TiO$_2$	335.6	1.96			–	–
0.50%Au−Pd/TiO$_2$(ED)	335.0	1.99	337.3	1.88	83.1	1.29
0.75%Au−Pd/TiO$_2$(ED)	335.0	1.86	337.5	1.97	83.3	1.17
1.10%Au−Pd/TiO$_2$(ED)	335.0	1.98	337.5	1.96	83.4	1.72
0.75%Au−Pd/TiO$_2$(IM)	336.4	1.97	338.2	1.90	84.7	1.75
0.12%Cu−Pd/TiO$_2$(ED)	335.2	1.97	337.6	1.90	–	–
0.28%Cu−Pd/TiO$_2$(ED)	335.5	1.99	338.2	1.99	–	–
0.30%Cu−Pd/TiO$_2$(IM)	336.5	1.97	338.1	1.98	–	–

of Pd. The former peak at 335.0 eV was attributed to the electronic effect between Pd and Au and the latter peak was assigned to Pd oxides. In addition, the peak of Au4f$_{7/2}$ was shifted to lower binding energy relative to the Au metal reference. The shift of binding energy of Pd3d and Au4f towards lower values has been reported to be due to an electron modification upon Au addition.[23,58,59] Comparing to the binding energy of Au metal reference, the shift in binding energy was found to decrease with Au coverage. The higher surface coverage of Au caused the autocatalytic deposition resulting in the formation of three-dimensional aggregates of Au on Pd, which are more similar to the Au metal particles.[37] The peak of Pd 3d for the Cu–Pd/TiO$_2$ catalysts was resolved into 2 peaks similarly to the Au–Pd/TiO$_2$ catalysts. The former peak of Pd3d suggested the electronic modification of Pd interacted with Cu and the latter was Pd oxides. On the other hands, the binding energy of Pd3d for the bimetallic catalysts prepared by IM indicated the presence of Pd oxide species consisting of PdO and PdO$_2$.[60] Like the Pd3d, the binding energy of Au4f for the Au–Pd/TiO$_2$ prepared by IM shifted to higher than the Au metal indicating the formation of Au oxides. The formation of Pd oxides and Au oxides found in the catalysts prepared by IM was likely because of the calcination step.

The typical TEM micrographs of the TiO$_2$ support, the monometallic Pd/TiO$_2$, and the bimetallic Au–Pd/TiO$_2$ and Cu–Pd/TiO$_2$ catalysts are shown in Figure 8. The TiO$_2$ support particles showed a spherical shape with the average crystallite size of 17–19 nm, which was consistent with the results determined from the XRD results. No change in crystallite size was found after SEA of Pd and ED of second metal. For the monometallic Pd catalyst prepared by SEA, the Pd or PdO was difficult to observe because of very small particle size of Pd/PdO or well-dispersion of Pd/PdO on TiO$_2$ supports. Nevertheless, some of the agglomeration of small metal particles could be seen after the deposition of second metal.

3.2 *Catalytic reaction results*

The catalytic performances of the prepared catalysts were investigated in the gas-phase selective hydrogenation of acetylene in excess ethylene at the temperature range of 40–100 °C. The acetylene conversion and ethylene selectivity are presented in Figures 9 and 10, respectively. For the Cu addition, the Cu–Pd/TiO$_2$ catalysts showed higher acetylene conversion and ethylene selectivity compared to Pd/TiO$_2$. The decrease in catalytic activity with Cu coverage was observed since some of Pd surface sites were covered by Cu as seen by the lower intensity of the CO-IR spectra. The ethylene selectivity increased with Cu addition. Typically, the second metal addition affected acetylene and ethylene adsorption mode on the catalyst surface that influenced the ethylene selectivity in the selective hydrogenation of acetylene. From the literature, ethylene can adsorb on isolated Pd atoms with a π-bonded mode and then easily desorb as ethylene because of relatively weak π-adsorption, whereas on the large Pd ensembles ethylene would adsorb with a multi-σ-bonded mode which is a strong adsorption and then could be fully hydrogenated to ethane if H$_2$ is present.[7,61] The adsorption mode of multi-σ-bonded species on Pd ensembles results in the formation of ethylidyne that undergoes sequential hydrogenation: ethylidyne → ethylidene → ethyle → ethane.[1,62,63] Moreover, the multi-σ-bonded ethylidyne on Pd ensembles has been reported to result in the catalyst fouling.[64] Thus, the adsorption mode of multi-σ-bonded ethylidyne should be suppressed in selective hydrogenation of acetylene. According to our CO-IR results, the ED of Cu on Pd catalysts could dilute the contiguous Pd, thus promoting the isolated Pd atoms. The results in this study suggest that change in the ensemble size of Pd surface atoms to isolated Pd atoms upon ED of Cu can alter the adsorption mode of multi-σ-bonded ethylidyne to π-bonded species, which promoted the desorption of ethylene, leading to the

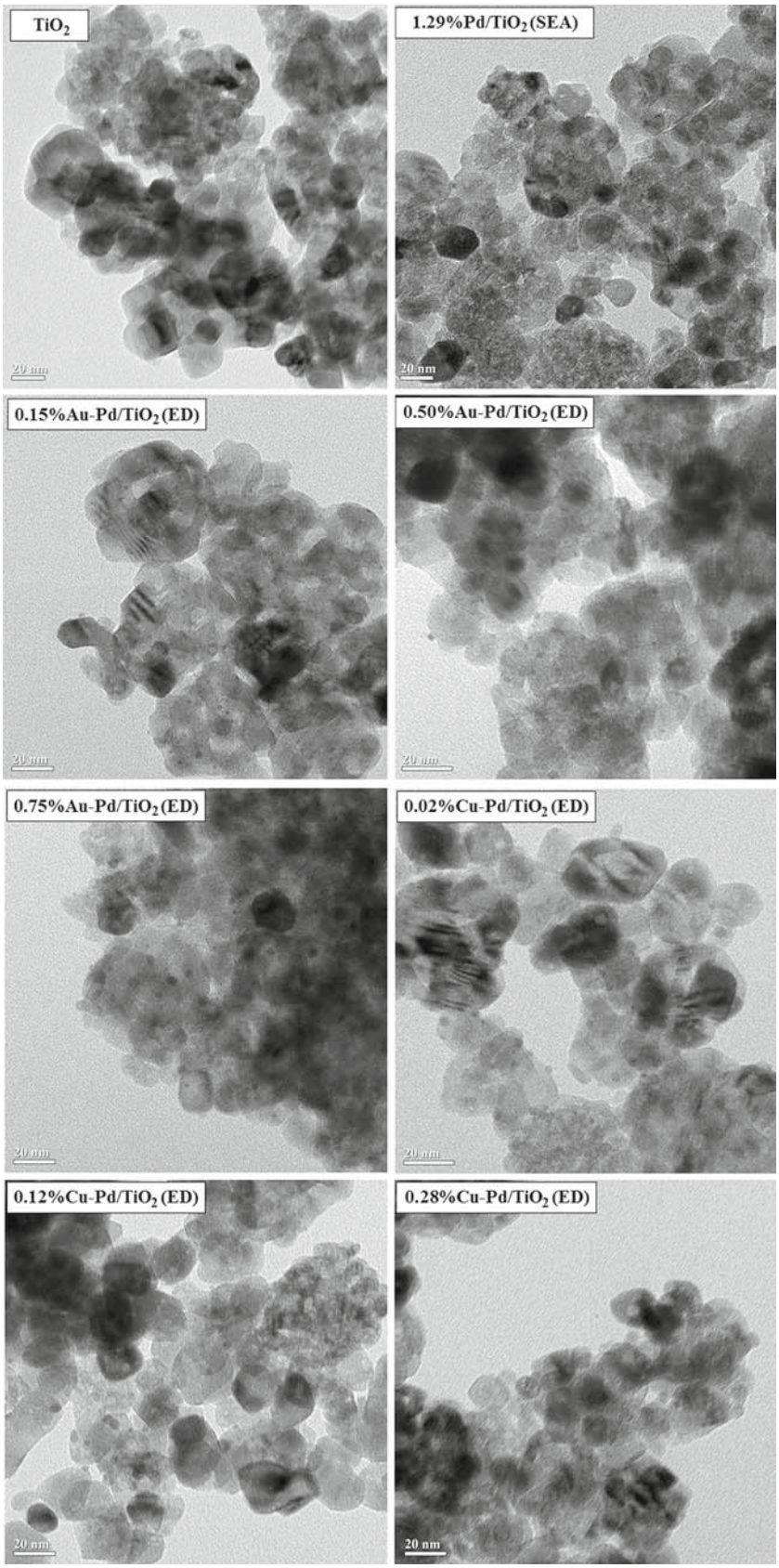

Figure 8. TEM images for commercial TiO_2 support, Pd/TiO_2, $Au-Pd/TiO_2$, and $Cu–Pd/TiO_2$ catalysts.

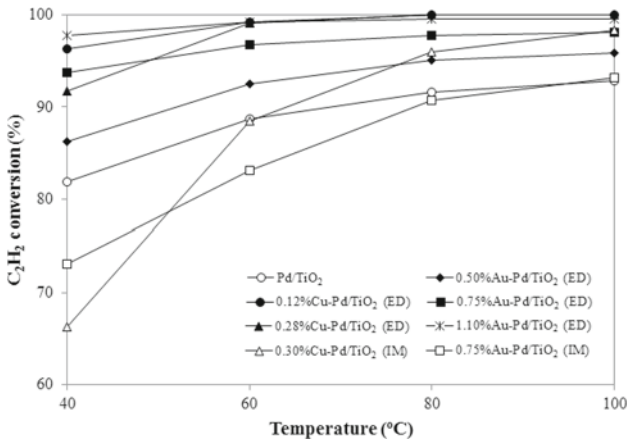

Figure 9. Acetylene conversion in selective hydrogenation of acetylene for Pd/TiO$_2$, Au−Pd/TiO$_2$, and Cu–Pd/TiO$_2$ catalysts.

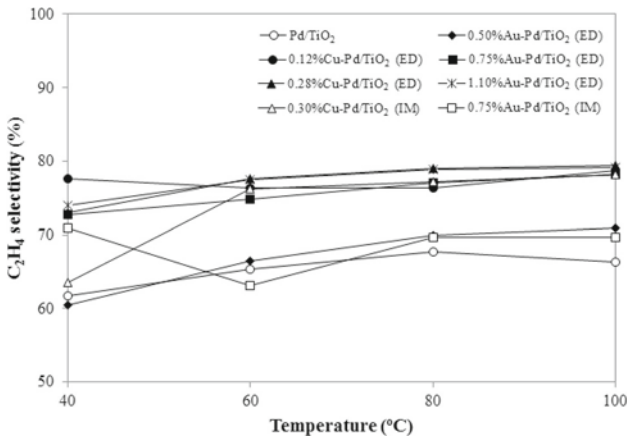

Figure 10. Ethylene selectivity in selective hydrogenation of acetylene for Pd/TiO$_2$, Au−Pd/TiO$_2$, and Cu–Pd/TiO$_2$ catalysts.

improvement of ethylene selectivity upon Cu addition.

Regarding the electronic effect, some studies found that Cu addition could modify the electronic structure of Pd surface by increasing the electron density of Pd, leading to weak adsorption of ethylene and promoting the H_2 dissociation.[20,21] However, the Cu addition by ED resulted in the blue shift (according to the CO-IR results), indicating that electron density on Pd surface atoms decreased upon Cu deposition by ED.[37] Such results suggested that the ensemble effect was more pronounced in our case in which Cu was added to the Pd/TiO$_2$ by ED.

For the Au addition by ED, the catalytic activity was found to increase with Au coverage. Considering the ensemble effect on the activity, the Pd dilution effect was assumed to be negligible because the relative ratio of linear and non-linear was not significantly changed. The performances of Au–Pd/TiO$_2$ catalysts were rather affected by the electronic modification upon Au addition as also revealed by the blue shift of both linear and non-linear bands in the CO-IR and the XPS results. It has been suggested that charge transfer from Pd to Au led to the formation of activated Au, which could adsorb hydrogen.[59,65–67] The selectivity of ethylene also increased upon Au addition despite its unchanged relative ratio of linear and non-linear species. However, the relative ratio of tri-coordinated CO adsorption mode was significantly decreased and the compressed-bridged and isolated-bridged mode was subsequently increased with Au coverage which suggested the decrease in Pd ensemble size, resulting in an improved ethylene selectivity.

The bimetallic catalysts prepared by impregnation showed lower catalytic activity than the Pd/TiO$_2$ and the bimetallic catalysts prepared by ED. The poor catalytic activity of the bimetallic catalyst prepared by IM was correlated to the lower relative ratio of the linear band which indicated to the presence of very low isolated Pd atoms. The addition of second metal by IM resulted in the coverage of Au or Cu aggregates on the Pd surface and the electronic property of the Pd-based catalysts was barely modified upon the second metal addition by IM.

4. Conclusions

The catalytic performances of Cu–Pd/TiO$_2$ and Au–Pd/TiO$_2$ catalysts for selective hydrogenation of acetylene in excess ethylene could be improved by using the combination of two methods including SEA for preparation of Pd catalysts and ED for second metal addition. The Cu addition by ED promoted the formation of isolated Pd atoms, as revealed by the CO-IR results. The ensemble effect was suggested to be responsible for the improvement of acetylene conversion and ethylene selectivity in the Cu–Pd/TiO$_2$ catalysts, rather than the electronic effect. However, Au addition by ED could not increase the isolated Pd atoms but the electronic modification could be observed from the CO-IR and XPS results. In addition, preparation of the bimetallic catalysts by using conventional impregnation method exhibited several drawbacks such as very low Pd dispersion, formation of second metal aggregates, and blockage of isolated Pd atoms, hence the catalyst exhibited poor catalytic performances.

Acknowledgements

Financial support from the Rachadapisek Sompote Fund for Postdoctoral Fellowship, Chulalongkorn University for B.P. and the Grant for International Research Integration:

Chula Research Scholar, and the Thailand Research Fund (BRG5780010) are gratefully acknowledged.

References

1. Zhang Y, Diao W, Williams C T and Monnier J R 2014 Selective hydrogenation of acetylene in excess ethylene using Ag- and Au–Pd/SiO_2 bimetallic catalysts prepared by electroless deposition *Appl. Catal. A: Gen.* **469** 419
2. Khan N A, Shaikhutdinov S and Freund H-J 2006 Acetylene and Ethylene Hydrogenation on Alumina Supported Pd–Ag Model Catalysts *Catal. Lett.* **108** 159
3. Zea H, Lester K, Datye A K, Rightor E, Gulotty R, Waterman W and Smith M 2005 The influence of Pd–Ag catalyst restructuring on the activation energy for ethylene hydrogenation in ethylene–acetylene mixtures *Appl. Catal. A: Gen.* **282** 237
4. Lam W K and Lloyd L 1972 Catalyst Aids Selective Hydrogenation of Acetylene *Oil Gas J.* **70** 66
5. Bond G C 1962 In *Catalysis by Metals* (London and New York: Academic Press) p. 281
6. Kim W-J and Moon S H 2012 Modified Pd catalysts for the selective hydrogenation of acetylene *Catal. Today* **185** 2
7. Riyapan S, Zhang Y, Wongkaew A, Pongthawornsakun B, Monnier J R and Panpranot J 2016 Preparation of improved Ag-Pd/TiO_2 catalysts using the combined strong electrostatic adsorption and electroless deposition methods for the selective hydrogenation of acetylene *Catal. Sci. Technol.* **6** 5608
8. Molnár Á, Sárkány A and Varga M 2001 Hydrogenation of carbon–carbon multiple bonds: chemo-, regio- and stereo-selectivity *J. Mol. Catal. A: Chem.* **173** 185
9. Trimm D L 1980 In *Design of Industrial Catalysts* (Amsterdam: Elsevier) p. 229
10. Zhang Q, Li J, Liu X and Zhu Q 2000 Synergetic effect of Pd and Ag dispersed on Al_2O_3 in the selective hydrogenation of acetylene *Appl. Catal. A: Gen.* **197** 221
11. Ma X-Y, Chai Y-Y, Evans D G, Li D-Q and Feng J-T 2011 Preparation and Selective Acetylene Hydrogenation Catalytic Properties of Supported Pd Catalyst by the in Situ Precipitation-Reduction Method *J. Phys. Chem. C* **115** 8693
12. Nikolaev S A, Zanaveskin L N, Smirnov V V, Averyanov V A and Zanaveskin K L 2009 Catalytic hydrogenation of alkyne and alkadiene impurities in alkenes. Practical and theoretical aspects *Russ. Chem. Rev.* **78** 231
13. Pei G X, Liu X Y, Wang A, Li L, Huang Y, Zhang T, Lee J W, Jang B W L and Mou C-Y 2014 Promotional effect of Pd single atoms on Au nanoparticles supported on silica for the selective hydrogenation of acetylene in excess ethylene *New J. Chem.* **38** 2043
14. Choudhary T V, Sivadinarayana C, Datye A K, Kumar D and Goodman D W 2003 Acetylene Hydrogenation on Au-Based Catalysts *Catal. Lett.* **86** 1
15. Leviness S, Nair V, Weiss A H, Schay Z and Guczi L 1984 Acetylene hydrogenation selectivity control on PdCu/Al_2O_3 catalysts *J. Mol. Catal.* **25** 131
16. Shu-ying Z, Rui-jun H and Tie-feng W 2012 Effects of Supports and Promoter Ag on Pd Catalysts for Selective Hydrogenation of Acetylene *Chin. J. Process Eng.* **12** 489
17. Sárkány A, Horváth A and Beck A 2002 Hydrogenation of acetylene over low loaded Pd and Pd-Au/SiO_2 catalysts *Appl. Catal. A: Gen.* **229** 117
18. Ota A, Armbrüster M, Behrens M, Rosenthal D, Friedrich M, Kasatkin I, Girgsdies F, Zhang W, Wagner R and Schlögl R 2011 Intermetallic Compound Pd_2Ga as a Selective Catalyst for the Semi-Hydrogenation of Acetylene: From Model to High Performance Systems *J. Phys. Chem. C* **115** 1368
19. Kang J H, Shin E W, Kim W J, Park J D and Moon S H 2000 Selective hydrogenation of acetylene on Pd/SiO_2 catalysts promoted with Ti, Nb and Ce oxides *Catal. Today* **63** 183
20. Pei G X, Liu X Y, Yang X, Zhang L, Wang A, Li L, Wang H, Wang X and Zhang T 2017 Performance of Cu-Alloyed Pd Single-Atom Catalyst for Semihydrogenation of Acetylene under Simulated Front-End Conditions *ACS Catal.* **7** 1491
21. Moon S H, Lee J H and Kim S K 2010, AIChE Annual Meeting, 8th November (Salt Lake City, UT)
22. Kim S K, Lee J H, Ahn I Y, Kim W-J and Moon S H 2011 Performance of Cu-promoted Pd catalysts prepared by adding Cu using a surface redox method in acetylene hydrogenation *Appl. Catal. A: Gen.* **401** 12
23. Pongthawornsakun B, Fujita S-i, Arai M, Mekasuwandumrong O and Panpranot J 2013 Mono- and bi-metallic Au–Pd/TiO_2 catalysts synthesized by one-step flame spray pyrolysis for liquid-phase hydrogenation of 1-heptyne *Appl. Catal. A: Gen.* **467** 132
24. Miller J T, Schreier M, Kropf A J and Regalbuto J R 2004 A fundamental study of platinum tetraammine impregnation of silica: 2. The effect of method of preparation, loading, and calcination temperature on (reduced) particle size *J. Catal.* **225** 203
25. Jiao L and Regalbuto J R 2008 The synthesis of highly dispersed noble and base metals on silica via strong electrostatic adsorption: I. Amorphous silica *J. Catal.* **260** 329
26. Jiao L and Regalbuto J R 2008 The synthesis of highly dispersed noble and base metals on silica via strong electrostatic adsorption: II. Mesoporous silica SBA-15 *J. Catal.* **260** 342
27. Lambert S, Job N, D'Souza L, Pereira M F R, Pirard R, Heinrichs B, Figueiredo J L, Pirard J-P and Regalbuto J R 2009 Synthesis of very highly dispersed platinum catalysts supported on carbon xerogels by the strong electrostatic adsorption method *J. Catal.* **261** 23
28. Cho H-R and Regalbuto J R 2015 The rational synthesis of Pt–Pd bimetallic catalysts by electrostatic adsorption *Catal. Today* **246** 143
29. Feltes T E, Espinosa-Alonso L, Smit E d, D'Souza L, Meyer R J, Weckhuysen B M and Regalbuto J R 2010 Selective adsorption of manganese onto cobalt for optimized Mn/Co/TiO_2 Fischer–Tropsch catalysts *J. Catal.* **270** 95
30. Liu X, Li Y, Lee J W, Hong C-Y, Mou C-Y and Jang B W L 2012 Selective hydrogenation of acetylene in excess ethylene over SiO_2 supported Au–Ag bimetallic catalyst *Appl. Catal. A: Gen.* **439** 8
31. Liu X, Mou C-Y, Lee S, Li Y, Secrest J and Jang B W L 2012 Room temperature O_2 plasma treatment of SiO_2 supported Au catalysts for selective hydrogenation of

acetylene in the presence of large excess of ethylene *J. Catal.* **285** 152
32. Duca D, Frusteri F, Parmaliana A and Deganello G 1996 Selective hydrogenation of acetylene in ethylene feedstocks on Pd catalysts *Appl. Catal. A: Gen.* **146** 269
33. Mekasuwandumrong O, Phothakwanpracha S, Jongsomjit B, Shotipruk A and Panpranot J 2011 Influence of flame conditions on the dispersion of Pd on the flame spray-derived Pd/TiO_2 nanoparticles *Powder Technol.* **210** 328
34. Thamaphat K, Limsuwan P and Ngotawornchai B 2008 Phase characterization of TiO_2 powder by XRD and TEM *Kasetsart J. (Nat. Sci.)* **42** 357
35. Hosseini M, Barakat T, Cousin R, Aboukaïs A, Su B L, De Weireld G and Siffert S 2012 Catalytic performance of core–shell and alloy Pd–Au nanoparticles for total oxidation of VOC: The effect of metal deposition *Appl. Catal. B: Environ.* **111–112** 218
36. Tiwari V, Jiang J, Sethi V and Biswas P 2008 One-step synthesis of noble metal–titanium dioxide nanocomposites in a flame aerosol reactor *Appl. Catal. A: Gen.* **345** 241
37. Rebelli J, Rodriguez A A, Ma S, Williams C T and Monnier J R 2011 Preparation and characterization of silica-supported, group IB–Pd bimetallic catalysts prepared by electroless deposition methods *Catal. Today* **160** 170
38. Schaal M T, Rebelli J, McKerrow H M, Williams C T and Monnier J R 2010 Effect of liquid phase reducing agents on the dispersion of supported Pt catalysts *Appl. Catal. A: Gen.* **382** 49
39. Ohno I, Wakabayashi O and Haruyama S 1985 Anodic Oxidation of Reductants in Electroless Plating *J. Electrochem. Soc.* **132** 2323
40. Giorgi J B, Schroeder T, Bäumer M and Freund H-J 2002 Study of CO adsorption on crystalline-silica-supported palladium particles *Surf. Sci.* **498** L71
41. Gelin P, Siedle A R and Yates J T 1984 Stoichiometric Adsorbate Species Interconversion Processes in the Chemisorbed Layer. An Infrared Study of the CO/Pd System *J. Phys. Chem.* **88** 2978
42. Xu X and Goodman D W 1993 An Infrared and Kinetic Study of CO oxidation on Model Silica-Supported Palladium Catalysts from 10^{-9} to 15 Torr *J. Phys. Chem.* **97** 7711
43. Li L, Zhao J, Yang J, Fu T, Xue N, Peng L, Guo X and Ding W 2015 A sintering-resistant Pd/SiO_2 catalyst by reverse-loading nano iron oxide for aerobic oxidation of benzyl alcohol *RSC Adv.* **5** 4766
44. Yudanov I V, Sahnoun R, Neyman K M, Rösch N, Hoffmann J, Schauermann S, Johánek V, Unterhalt H, Rupprechter G, Libuda J and Freund H-J 2003 CO Adsorption on Pd Nanoparticles: Density Functional and Vibrational Spectroscopy Studies *J. Phys. Chem. B* **107** 255
45. Wolter K, Seiferth O, Libuda J, Kuhlenbeck H, Bäumer M and Freund H J 1998 Infrared study of CO adsorption on alumina supported palladium particles *Surf. Sci.* **402–404** 428
46. Szanyi J, Kuhn W K and Goodman D W 1993 CO adsorption on Pd(111) and Pd(100): Low and high pressure correlations *J. Vac. Sci. Technol. A* **11** 1969
47. Wadayama T, Abe K and Osano H 2006 Infrared reflection absorption study of carbon monoxide adsorption on Pd/Cu(1 1 1) *Appl. Surf. Sci.* **253** 2540
48. Bradshaw A M and Hoffmann F M 1978 The chemisorption of carbon monoxide on palladium single crystal surfaces: IR spectroscopic evidence for localised site adsorption *Surf. Sci.* **72** 513
49. Rebelli J, Detwiler M, Ma S, Williams C T and Monnier J R 2010 Synthesis and characterization of Au–Pd/SiO_2 bimetallic catalysts prepared by electroless deposition *J. Catal.* **270** 224
50. Sá J, Gross S and Vinek H 2005 Effect of the reducing step on the properties of Pd–Cu bimetallic catalysts used for denitration *Appl. Catal. A: Gen.* **294** 226
51. Hadjiivanov K, Tsoncheva T, Dimitrov M, Minchev C and Knözinger H 2003 Characterization of Cu/MCM-41 and Cu/MCM-48 mesoporous catalysts by FTIR spectroscopy of adsorbed CO *Appl. Catal. A: Gen.* **241** 331
52. Fernández-García M, Anderson J A and Haller G L 1996 Alloy Formation and Stability in Pd–Cu Bimetallic Catalysts *J. Phys. Chem.* **100** 16247
53. Pawelec B, Venezia A M, La Parola V, Cano-Serrano E, Campos-Martin J M and Fierro J L G 2005 AuPd alloy formation in Au–Pd/Al_2O_3 catalysts and its role on aromatics hydrogenation *Appl. Sci.* **242** 380
54. Kugler E L and Boudart M 1979 Ligand and ensemble effects in the adsorption of carbon monoxide on supported palladium–gold alloys *J. Catal.* **59** 201
55. Venezia A M, La Parola V, Deganello G, Pawelec B and Fierro J L G 2003 Synergetic effect of gold in Au/Pd catalysts during hydrodesulfurization reactions of model compounds *J. Catal.* **215** 317
56. Jin M, Park J-N, Shon J K, Kim J H, Li Z, Park Y-K and Kim J M 2012 Low temperature CO oxidation over Pd catalysts supported on highly ordered mesoporous metal oxides *Catal. Today* **185** 183
57. Beck A, Horváth A, Schay Z, Stefler G, Koppány Z, Sajó I, Geszti O and Guczi L 2007 Sol derived gold–palladium bimetallic nanoparticles on TiO_2: structure and catalytic activity in CO oxidation *Top. Catal.* **44** 115
58. Lee Y S, Jeon Y, Chung Y D, Lim K Y, Whang C N and Oh S J 2000 Charge Redistribution and Electronic Behavior in Pd–Au Alloys *J. Korean. Phys. Soc.* **37** 451
59. Pongthawornsakun B, Mekasuwandumrong O, Prakash S, Ehret E, Santos Aires F J C and Panpranot J 2015 Effect of reduction temperature on the characteristics and catalytic properties of TiO_2 supported AuPd alloy particles prepared by one-step flame spray pyrolysis in the selective hydrogenation of 1-heptyne *Appl. Catal. A: Gen.* **506** 278
60. Qi B, Di L, Xu W and Zhang X 2014 Dry plasma reduction to prepare a high performance Pd/C catalyst at atmospheric pressure for CO oxidation *J. Mater. Chem. A* **2** 11885
61. Lee J H, Kim S K, Ahn I Y, Kim W-J and Moon S H 2012 Performance of Ni-added Pd–Ag/Al_2O_3 catalysts in the selective hydrogenation of acetylene *Korean J. Chem. Eng.* **29** 169

62. Wood J, Alldrick M J, Winterbottom J M, Stitt E H and Bailey S 2007 Diffuse reflectance infrared Fourier transform spectroscopy (DRIFTS) study of ethyne hydrogenation on Pd/Al_2O_3 *Catal. Today* **128** 52
63. Margitfalvi J, Guczi L and Weiss A H 1981 Reaction routes for hydrogenation of acetylene–ethylene mixtures using a double labelling method *React. Kinet. Catal. L.* **15** 475
64. Mei D, Neurock M and Smith C M 2009 Hydrogenation of acetylene–ethylene mixtures over Pd and Pd–Ag alloys: First-principles-based kinetic Monte Carlo simulations *J. Catal.* **268** 181
65. Chen Y and Lee D 2013 Liquid Phase Hydrogenation of *p*-Chloronitrobenzene on Au-Pd/TiO_2 Catalysts: Effects of Reduction Methods *Mod. Res. Catal.* **2** 25
66. Goodman D W 2005 "Catalytically active Au on Titania:" yet another example of a strong metal support interaction (SMSI)? *Catal. Lett.* **99** 1
67. Schimpf S, Lucas M, Mohr C, Rodemerck U, Brückner A, Radnik J, Hofmeister H and Claus P 2002 Supported gold nanoparticles: in-depth catalyst characterization and application in hydrogenation and oxidation reactions *Catal. Today* **72** 63